Pool Boiling Behavior and Critical Heat Flux on Zircaloy and SiC Claddings in Deionized Water under Atmospheric Pressure

Gwang Hyeok Seo, Gyoodong Jeun, Sung Joong Kim *
Department of Nuclear Engineering, Hanyang University
222 Wangsimni-ro, Seongdong-gu, Seoul, 133-791, Republic of Korea
**Corresponding author: sungjkim@hanyang.ac.kr*

1. Introduction

Recently, an importance in adopting new fuel claddings have been emerged. For more efficiently advanced operation of nuclear reactors, many researchers have suggested improved fuel claddings in terms of extended fuel cycle and high burnup fuels. Furthermore, a great interest in the enhanced reactor safety has been paid attention, especially since the Fukushima Daiich accident occurred. In this sense, Silicon Carbide (SiC) has been attractive for nuclear application as an accident tolerant fuel cladding. SiC cladding shows noticeable advantages in aspects of better high-temperature corrosion properties, safety and best waste disposal restriction, greater high-temperature strength, lower effective neutron cross section, etc. [1]. Most of all, one remarkable profit of adopting the SiC cladding as compared to current zircaloy application is less hydrogen generation during severe accident sequences as well as during the normal operation [2].

Recently, several researches on SiC material as an alternative of the nuclear fuel cladding have been conducted. From a fundamental point of view, Snead et al. did an extensive investigation on SiC properties [3]. Their work revealed non-irradiated and irradiated material properties. In addition to the existing literature data, they even added new data, particularly in the high-temperature irradiation regime. Moreover, Carpenter has studied performance of a SiC fuel cladding in his Ph. D. thesis [4]. With extensive in-core tests at MITR-II, his works showed the effects of cladding design for monolith and triplex types. He concluded that manufacturing techniques of the SiC cladding affected corrosion rates and swelling behavior after irradiation. For more practical nuclear applications, oxidation rates of a SiC cladding was investigated with a comparison assessment of those of a zircaloy-4 cladding. Lee et al. adopted an oxidation process under the conditions of the Loss of Coolant Accidents (LOCA) in LWRs [5]. They found that SiC oxidation rates were greatly lower than those of zircaloy-4.

In order to demonstrate the superiority of SiC cladding in terms of thermal performance, in this study pool boiling heat transfer experiments were carried out in a pool of saturated deionized water (DI water) at atmospheric pressure. For a comparison study, zircaloy-4 claddings, which are current fuel claddings in LWRs, were used as a reference case. Not only measuring nucleate boiling heat transfer coefficient (NBHTC) and critical heat flux (CHF) but also observing boiling behavior of both the claddings were conducted.

2. Experimental

2.1 Description of Experimental Apparatus and Heater Design

The experiments were carried out in order to investigate the boiling heat transfer performance of zircaloy and SiC claddings in a pool of saturated DI water under atmospheric pressure. Since pool boiling experiment is usually accompanied by visualization work, four windows are provided with quartz, which provides the best opportunity for visualization of boiling. A schematic of pool boiling facilities used in this study are shown in Fig. 1.

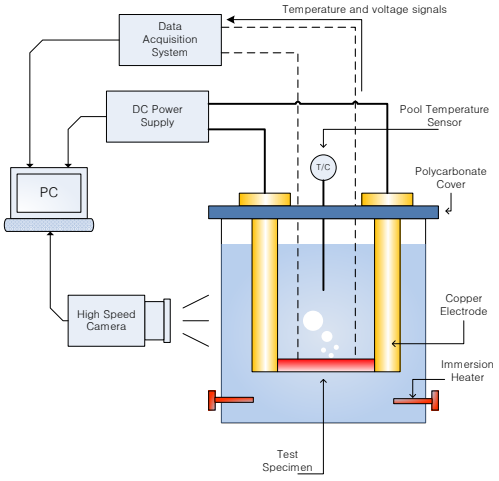

Fig. 1 Pool boiling isothermal bed

Two types of heaters are used in this study. As a reference case, a zircaloy-4 tube heater assembly was prepared. Figure 2 shows a schematic of the zircaloy heater assembly. The zircaloy-4 tube was mechanically connected by the cylindrical copper electrodes, which supplied electrical power to the zircaloy heater. Diameter and length of the zircaloy heater are 9.5 mm and 50.8 mm, respectively. In order to measure wall temperature, three K-type TCs wrapped by metal foil were attached to the inner wall of zircaloy tube in 90° azimuthally.

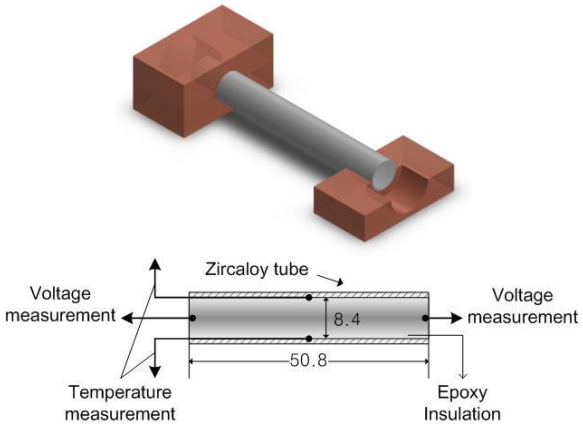

Fig. 2 Schematic of zircaloy heater assembly

Unlike the zircaloy heater assembly, design of SiC heater assembly is rather complicated because direct heating of SiC was not viable in this study and thus, an indirect heating method was employed. It consists of a stainless steel grade 316 (SS316) tube inside, an indium gap filler, and a SiC monolith tube as shown in Fig. 3. As a result, a SiC heater assembly is designed very similar to the design of a real fuel rod. Diameter and length of SiC monolith tube are 10.2 mm and 50.8 mm, respectively. The thermocouple of the SiC heaters is positioned in the gap between the SiC tube and the inner SS316 tube, and at the center of the inner SS316 tube. The SiC monolith tubes were obtained by generous donation from GAMMA CTP.

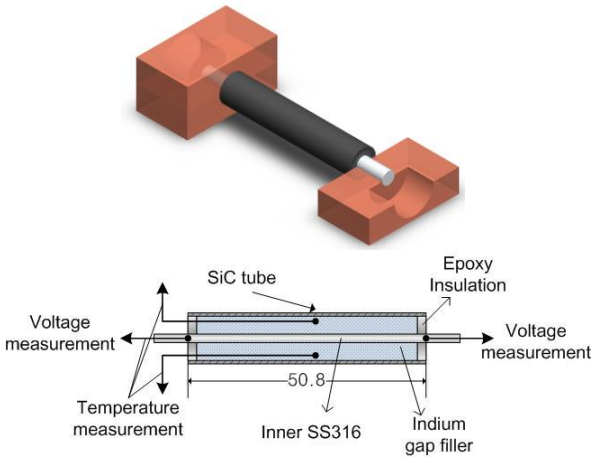

Fig. 3 Schematic of SiC heater assembly

2.2 Test Procedure

The pool boiling heat transfer experiment was conducted by applying the following procedures. In a heater preparation and preheating stage, a tube heater instrumented with a K-type TC and voltage taps was placed in the pool of water. The pool of water was then heated using two immersion type heaters until boiling occurred at atmospheric pressure.

While boiling the pool, with a very low current input, the electrical load was applied in a steady manner. At every heat flux increment of approximately 30 kW/m^2, a steady temperature and voltage were obtained. At the same time, the boiling phenomena were captured using a high-speed video camera (Phantom V7.3) at a photographing rate of 1,500 frames/sec.

Approaching the CHF, vigorous bubble departure and unstable vapor columns were observed. The CHF was determined to occur when a rapid temperature excursion was observed and/or by capturing the transition from nucleate boiling to film boiling. The CHF value was then determined as the average value between the previous step and current step which triggered the CHF. A typical power increase curve and detection of the CHF is shown in Fig. 4.

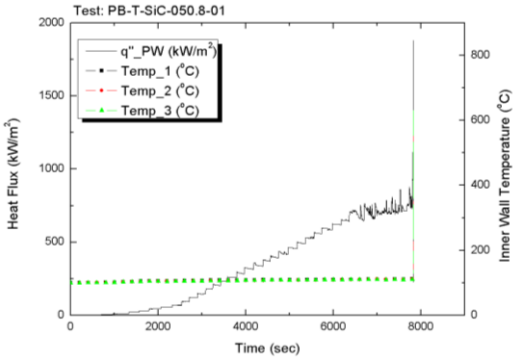

Fig. 4 The heat flux and inner wall temperature as a function of time for the SiC heater

2.3 Surface Characterization

The contact angle is an indicator used to quantify the surface wettability effect, which is a dominant parameter affecting the boiling heat transfer characteristics [6]. In order to evaluate the wettability of the employed test heaters, a static contact angle measurement was performed. Figure 5 shows pictures of the contact angles on the zircaloy and SiC tubes. The apparent contact angles on the heaters were estimated to be 85^o and 93^o for the zircaloy and SiC tubes, respectively, which suggests that only a slight difference of 8^o exists between the two heaters.

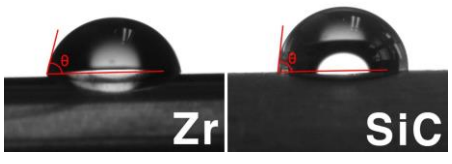

Fig. 5 Apparent contact angles: zircaloy: 85^o (left) and SiC: 93^o (right)

In addition to the contact angle measurements, the surface roughnesses of both heater surfaces were obtained. Surface roughness is also a key parameters

which affects the nucleate boiling heat transfer since it can be closely related to the number of micro-cavities. There is a greater chance of increased boiling heat transfer for a surface with a higher roughness value [7]. As a result, the surface roughness may affect the CHF. The Ramilison's CHF correlation presented in Eq. (1) indicates that a higher CHF is expected for a rougher heating surface.

$$q''_{crit} = 0.0366(\pi - \beta_r)^{3.0} R_q^{0.125} \times \frac{\pi}{24}\left[h_{fg}\rho_v^{1/2}\left\{\sigma g(\rho_l - \rho_v)\right\}^{1/4}\right]^{1/2} \quad (1)$$

Figure 6 shows the measured surface roughnesses of the zircaloy and SiC heaters. The arithmetic averages of the absolute values of the surface feature heights for the zircaloy and SiC tubes, Ra, were 88 and 107 nm, respectively. The measured roughness of the SiC tube is about 22 % higher than that of the zircaloy tube.

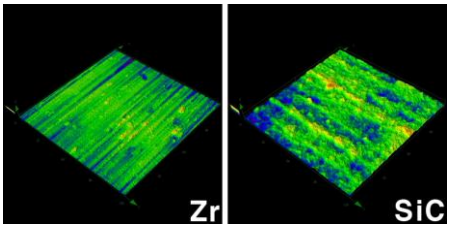

Fig. 6 Surface roughness, Ra [nm]: zircaloy: 88 (left) and SiC: 107 (right)

3. Results and Discussion

3.1 Critical Heat Flux of the Zircaloy-4 Cladding

As a reference case, experiments of three zircaloy-4 heaters were conducted in a pool of saturated DI water under atmospheric pressure. The resulting CHF values obtained in the experiments are presented in Table 1. The average CHF of the zircaloy-4 claddings was 684 kW/m^2.

Table 1: Summary of CHF values for zircaloy and SiC heaters

Test No.	CHF_Zr (kW/m^2)	CHF_SiC (kW/m^2)
Test 1	650	1,105
Test 2	648	899
Test 3	753	1,108
Average	684±35	1,037±69

The obtained CHF values were evaluated with several existing models relevant to the heater conditions. As important facts, the test heaters has a cylindrical geometry and specific surface conditions which were mentioned in the Chapter 2. Although Zuber's model (1959) shown in Eq. (2) is widely known as a conventional CHF correlation, it was developed for an infinite flat heater [8,9].

$$q''_{crit} = Ch_{fg}\rho_v^{1/2}\left[\sigma g(\rho_l - \rho_v)\right]^{1/4} \quad (2)$$

Here, the coefficient C is $\pi/24$ (= 0.13) and the Zuber's prediction provides a CHF value of 1,107 kW/m^2.

Since the test sample heaters have the geometry of a horizontal tube, other CHF models with geometrical considerations could be useful to compare the experimental results. Sun and Lienhard (1970) developed a CHF correlation including the effects of a heater diameter [8,9]. They introduced a dimensionless heater radius, R', as defined by Eq. (3).

$$R' = R\sqrt{\frac{g(\rho_l - \rho_v)}{\sigma}} \quad (3)$$

In the current study, the constant R' was evaluated to be 1.90. The CHF correlation for small cylinders (0.2 < R' < 2.4) based on their analysis is suggested by Eq. (4).

$$q''_{crit} = 0.123h_{fg}\rho_v^{1/2}\left[\frac{\sigma^3 g(\rho_l - \rho_v)}{R^2}\right]^{1/8} \quad (4)$$

Their model predicts a CHF value of 887 kW/m^2 for the zircaloy heaters. This result indicates that, for a small cylinder geometry, the CHF value with the effect of cylindrical geometry becomes lower than the Zuber's hydrodynamic limit. Although the difference between the predicted and the measured CHF values is 203 kW/m^2, the correlation with the geometrical effect demonstrates the tendency of decreasing CHF in the experiments.

In addition to the heater geometry, surface wettability is also an important parameter in understanding CHF phenomenon. Liaw and Dhir (1986) observed that the CHF decreased with increasing contact angle in the range of 27° to 107° [9]. They adopted the Zuber's model as a reference, and determined the constant C in the correlation suggested with the empirical results, as shown in Fig. 7. Using the contact angle data (85°) of the current zircaloy heater, a CHF value of 556 kW/m^2 is predicted, which is almost half the value obtained using Zuber's prediction. This value is close to our measured CHF of 684 kW/m^2, as shown in Table 1.

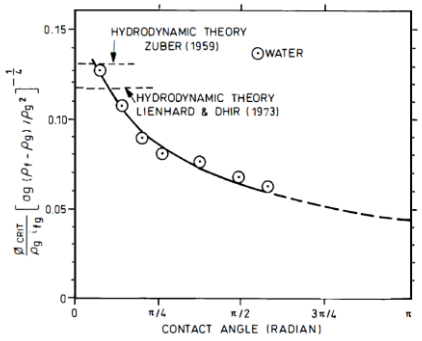

Fig. 7 CHF prediction as a function of the contact angle [9]

More explicitly, Kandlikar's model (2001) incorporates the effects of the surface contact angle, as shown in Eq. (5) [10].

$$q''_{crit} = h_{fg}\rho_v^{1/2}\left(\frac{1+\cos\beta}{16}\right)\left[\frac{2}{\pi}+\frac{\pi}{4}(1+\cos\beta)\cos\phi\right]^{1/2} \times\left[\sigma g(\rho_l-\rho_v)\right]^{1/4} \quad (5)$$

Here, β and ϕ are the surface contact angle and heater orientation angle, respectively. The Kandlikar's model predicted a CHF value of 702 kW/m^2 as the contact angle data of 85^o was used. The difference between the measured CHF and the prediction is only 18 kW/m^2. Figure 8 shows the experimental results of the zircaloy heaters with the suggested CHF predictions. Consequently, it is believed that the measured CHF is reasonable and the experiments were conducted successfully when considering the geometry or wettability effects.

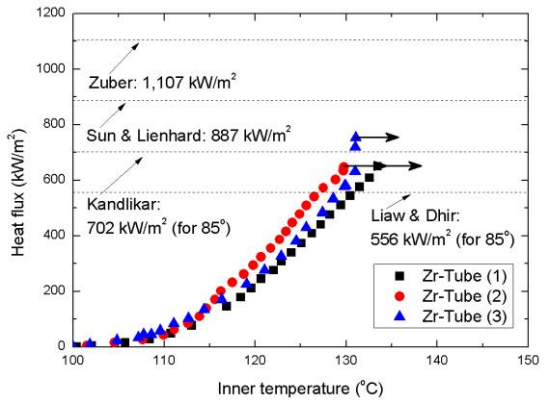

Fig. 8 . Comparison of measured and predicted CHF values for the zircaloy heaters

3.2 Comparison of the CHF Data of the Zircaloy-4 and SiC Claddings

Similar to the zircaloy-4 claddings, experiments of three SiC monolith claddings were conducted. As presented in Table 1, the average CHF of the SiC claddings is 1,037 kW/m^2, which is 52% higher than that of the zircaloy-4 claddings.

Figure 9 shows the boiling curves where the applied heat flux is plotted as a function of the inner wall temperatures of the zircaloy and SiC claddings. Two noticeable differences between the boiling curves exist. First, as the higher CHF of the SiC heater indicates, the points at which departure from nucleate boiling occurs are in the upper region for the SiC heaters compared to those of the zircaloy heaters.

Second, the slopes of the SiC claddings are steeper than those of the zircaloy claddings, which indicates better nucleate boiling heat transfer with the SiC claddings. One possible explanation for this preferable nucleate boiling is the surface roughness effect. As discussed in Section 2.3, the higher surface roughness was estimated for the SiC claddings compared to the zircaloy cladding. With the higher surface roughness, more micro-cavities are likely to be present and thus, these more micro-cavities can be nucleated with the SiC claddings. In addition to the surface roughness effect, the thermo-physical properties of the SiC cladding may contribute to the enhanced nucleate boiling. As shown in Table 2, the thermal conductivity of the SiC cladding is much higher than that of the zircaloy-4 cladding. Given the same applied heat flux, the wall temperature will be lower with a high thermal conductivity material due to the enhanced thermal dissipation.

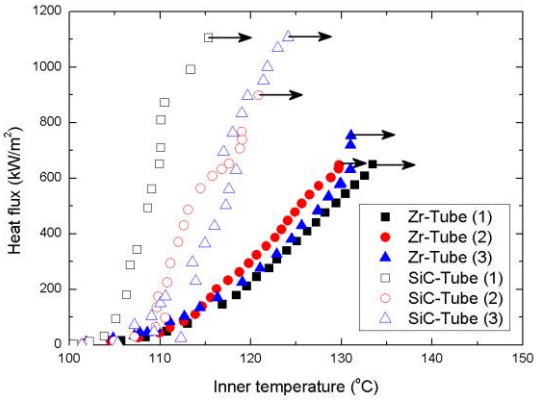

Fig. 9 Boiling curve of zircaloy and SiC heaters

Table 2: Thermo-physical properties of the zircaloy-4 and SiC claddings

	Zircaloy-4	SiC
ρ (kg/m^3)	6,560	3,210
k (W/m·K)	13.6	389.4
c_p (J/kg·K)	285	585
α×10^{-6} (J/m^2·K)	7.23	207.24
T_{melt} (^{o}C)	1,850	2,797

A similar observation was reported by aus der Wiesche et al. (2011) [11]. They discussed that although the heater geometry is different, a slower temperature variation of the heat flux was observed for the heater with a higher thermal conductivity, as shown in Fig. 10.

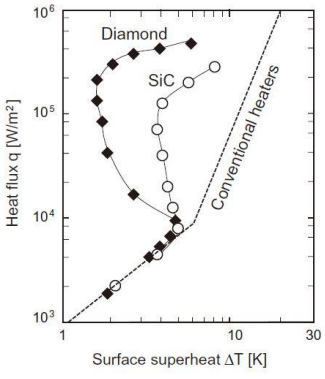

Fig. 10 Boiling curves for diamond and SiC heaters [11]

3.3 Visual observation of Zircaloy-4 and SiC heaters

Visual observation of the pool boiling heat transfer characteristics of zircaloy and SiC heaters was

conducted using a high-speed video system (HVS). The visualization work was focused on capturing the characteristic boiling phenomena of distinctive bubble dynamics during the nucleate boiling regime and the transition of boiling phenomenon from nucleate boiling to film boiling.

Figure 11 shows high speed images of zircaloy and SiC heaters until the CHF occurrence. The boiling pictures show typical fundamental boiling phenomena summarized by Zuber. In the low and moderate heat flux regions, isolated bubbles were mainly observed for both heaters. As the heat flux was increased, nucleate boiling developed. In this region, as Zuber's hydrodynamic theory explains, each bubble combines with neighboring ones and a vapor column forms.

However, as the heat flux was increased further up to about 340 kW/m^2, a distinct difference in the boiling mode was observed. For the zircaloy heater, a previous vapor column merges with a new column and the heater surface is covered with vapor blankets. Finally, boiling crisis at the heater surface takes place in a very short time interval when most surfaces of the heaters are covered with the vapor blankets. On the other hand, for the SiC cladding, even at a high heat flux addition of about 500 kW/m^2, isolated bubbles are still observed while the bubble size increases. Also, the bubble departure diameters from the SiC heater surface tend to be smaller than those from the zircaloy heater. As a result, the chance of vapor merge and coalescence for the SiC heater seems to be smaller than for the zircaloy heater and therefore, a higher CHF value is obtained.

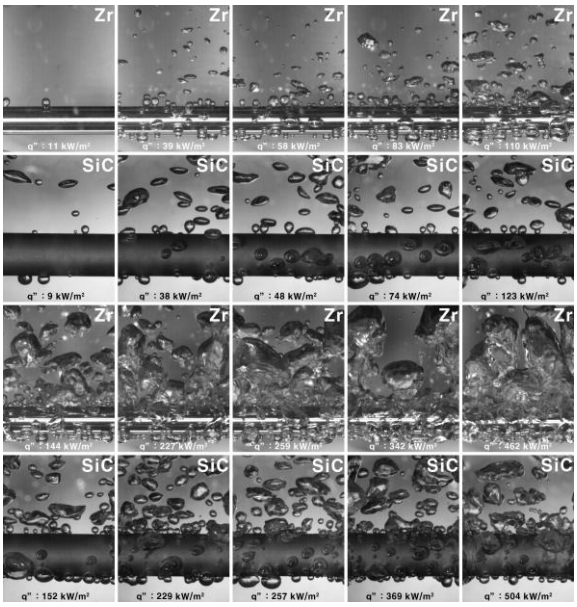

Fig. 11 High speed images of zircaloy and SiC heaters with a variation of heat flux

Figure 12 shows a comparison of the boiling phenomena of the zircaloy cladding and SiC heaters at the instantaneous moment of CHF occurrence. For the zircaloy-4 cladding, near the CHF, unstable vapor columns were formed and the entire heater was covered by a crowd of vapors. Right after the CHF was triggered, the zircaloy-4 heater started to glow due to instantaneous thermal insulation by the vapor and physical rupture occurred. For the SiC cladding, similar hydrodynamic instability as the zircaloy heater was observed near the CHF condition. However, the SiC was thermally very resistant to the high temperature and structurally intact even after the CHF where no physical damage occurred. As observed in Fig. 12(b), stable film boiling was maintained for several seconds because the SiC heater is thermally tolerant against the high temperature.

In addition, it should be noted that the experiments for the SiC heaters was terminated when the inner stainless steel heater element melted. The melting temperature of the SiC cladding (T_{melt} ~2,800ºC) is much higher than that of the heating element of the SS316 tube (T_{melt} ~1,400ºC). Thus, before the surface temperature of the SiC cladding exceeds its melting temperature, the inner heater element was destroyed upon the CHF and the experiment was terminated.

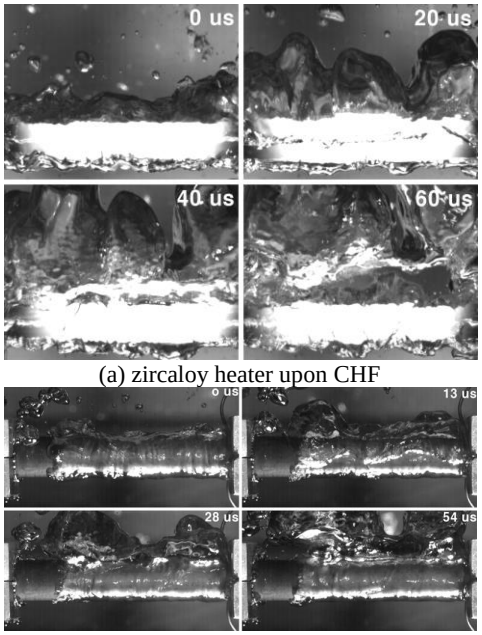

(a) zircaloy heater upon CHF

(b) SiC heater upon CHF

Fig. 12 Boiling behavior at the occurrence of CHF

One of the noticeable results in this experiment, in addition to the higher CHF with the SiC tube, is the structural integrity changes of both types of heaters after experiencing the CHF. In general, after CHF occurs, for most metallic materials such as stainless steel or zircaloy, the heating surface fails to maintain its structure. Figure 13 shows a visual comparison of the structural integrity for both types of heaters before and after the tests. The zircaloy claddings easily failed upon the CHF and were split into two or more fragments. On the other hand, the heater structure of the SiC claddings was maintained after the CHF although the film boiling

was established around both surfaces, as shown in Fig. 12.

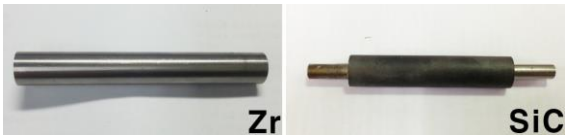

(a) zircaloy (left) and SiC (right) heaters before testing

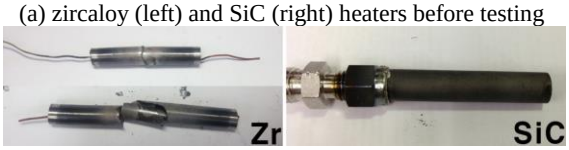

(b) zircaloy (left) and SiC (right) heaters after testing

Fig. 13 Change of the structural integrities of the zircaloy and SiC heaters before and after experiencing the CHF

As a candidate cladding material, this result implies that SiC has a great advantage in a nuclear power plant because adopting SiC material could provide relieved criteria in the reactor operation. Furthermore, from the aspect of the reactor safety in accident management, the feature of structural integrity with the CHF helps to allow more time to handle accidents since the cladding structure is a barrier for containing nuclear fuel fission fragments. Thus, the sustainable structure of SiC upon the CHF may provide an important advantage for nuclear reactor safety.

4. Conclusions

In this study, pool boiling heat transfer experiments with zircaloy and SiC heaters were carried out. Comparison of the CHF and nucleate boiling heat transfer of the zircaloy-4 and SiC cladding were compared. Specifically, sophisticated high-speed photographs of nucleate boiling, the CHF, and film boiling phenomena were captured. The major findings observed from this study can be summarized as follows.

- The experimental results showed a 52% higher CHF for the SiC heaters than the zircaloy heaters. This can be attributed to the high thermal conductivity and higher nucleate site density compared to those of the zircaloy-4 cladding.
- Boiling curves developed for the zircaloy-4 and SiC claddings suggest that better nucleate boiling heat transfer is attainable with the SiC cladding, which could be due to the higher surface roughness and higher thermal conductivity compared to those of the zircaloy-4 cladding.
- Structural integrity of the SiC heaters was preserved even after experiencing the CHF whereas the zircaloy heaters failed and were fragmented. This demonstrates the superiority of the SiC cladding in terms of the improved safety margin for nuclear applications and resistance to severe accidents during transient conditions.

Acknowledgements

This work was supported by the National Research Foundation of Korea (NRF) grant funded by Ministry of Science, ICT and Future Planning (MSIP) with grant number, 2012M2B2A6029184. The authors also greatly acknowledge Dr. Herb Feinroth in GAMMA CTP for generous donation for SiC monolith tube.

REFERENCES

[1] C. R. F. Azevedo, Selection of fuel cladding material for nuclear fission reactors, Engineering Failure Analysis, Vol. 18, pp. 1943-1962, 2011.
[2] L. Hallstadius, S. Johnson, and E. Lahoda, Cladding for high performance fuel, Progress in Nuclear Energy, Vol. 57, pp. 71-76, 2012.
[3] L. L. Snead, T. Nozawa, Y. Katoh, T. S. Byun, Kondo, S., and D. A. Petti, Handbook of SiC Properties for Fuel Performance Modeling, Journal of Nuclear Materials, Vol. 371, pp. 329-377, 2007
[4] D. M. Carpenter, An Assessment of Silicon Carbide as a Cladding Material for Light Water Reactors, PhD Dissertation, MIT Nuclear Science and Engineering June 2010.
[5] Y. Lee, T. J. McKrell, C. Yue, and M. S. Kazimi, Safety assessment of SiC cladding oxidation under Loss-Of-Coolant Accident conditions in light water reactors, Nuclear Technology, Vol. 183, pp. 210-227, 2013.
[6] S.J. Kim, I.C. Bang, J. Buongiorno, L.W. Hu, Surface wettability change during pool boiling of nanofluids and its effect on critical heat flux, International Journal of Heat and Mass Transfer, Vol. 50, pp. 4105–4116, 2007
[7] H. O'Hanley, C. Coyle, J. Buongiorno, T. McKrell, L.-W. Hu, M. Rubner, and R. Cohen, Separate effects of surface roughness, wettability, and porosity on the boiling critical heat flux. Applied Physics Letters, Vol. 103, p. 024102, 2013.
[8] L. S. Tong and Y. S. Tang, Boiling Heat Transfer and Two-Phase Flow, 2nd Ed., Taylor and Francis, 1997.
[9] J. G. Collier and J. R. Thome, Convective Boiling and Condensation, 3rd Ed., Oxford Science Publication, 1994.
[10] S. G. Kandlikar, A Theoretical Model to Predict Pool Boiling CHF Incorporating Effects of Contact Angle and Orientation, Journal of Heat Transfer, Vol. 123, pp. 1071-1079, 2001.
[11] S. aus der Wiesche, U. Bardas, and S. Uhkötter, Boiling heat transfer on large diamond and SiC heaters: The influence of thermal wall properties. International Journal of Heat and Mass Transfer, Vol. 54, pp. 1886-1895, 2011.